Electronic Supplementary Material (ESI) for CrystEngComm

Electronic Supplementary Information

Effect of substrate pre-treatment on controllable synthesis of hexagonal WO_3 nanorod arrays and their electrochromic properties

Feng Zheng, Hui Lu, Min Guo*, Mei Zhang

1. Effect of substrate pre-coating with WO_3 seed layers

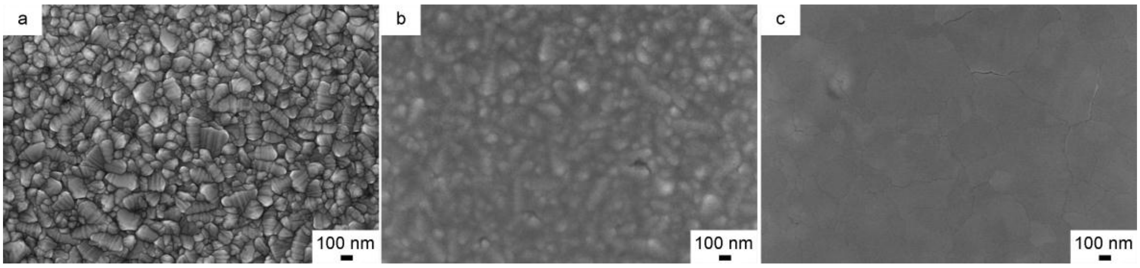

Fig. S1. SEM images of FTO substrates with different substrate pre-treatments: (a) unmodified FTO substrate, (b) pre-coated with 0.5 mol L^{-1} colloid solution for three times without annealing, (c) pre-coated with 0.5 mol L^{-1} colloid for three times, then annealed at 500 °C.

Fig. S1 shows the SEM images of FTO substrates with or without pre-coated WO_3 seed layers. The morphology of the bare FTO substrate surface can be clearly seen without pre-coating as shown in Fig. S1 (a). The FTO substrate is covered by a thin amorphous film when the substrate is spin coated for three times without annealing, and in the meantime, the FTO substrate surface still can be seen vaguely in Fig. S1 (b). However, it is shown from Fig. S1 (c) that the FTO substrate is covered by a layer of compact thin film when the substrate is spin coated for three times after

Department of Physical Chemistry, School of Metallurgical and Ecological Engineering, University of Science and Technology Beijing, Beijing 100083, P. R. China;
E-mail: guomin@ustb.edu.cn, Fax: +86 10 62334926

annealing.

2. Effect of annealing temperature (seed layers)

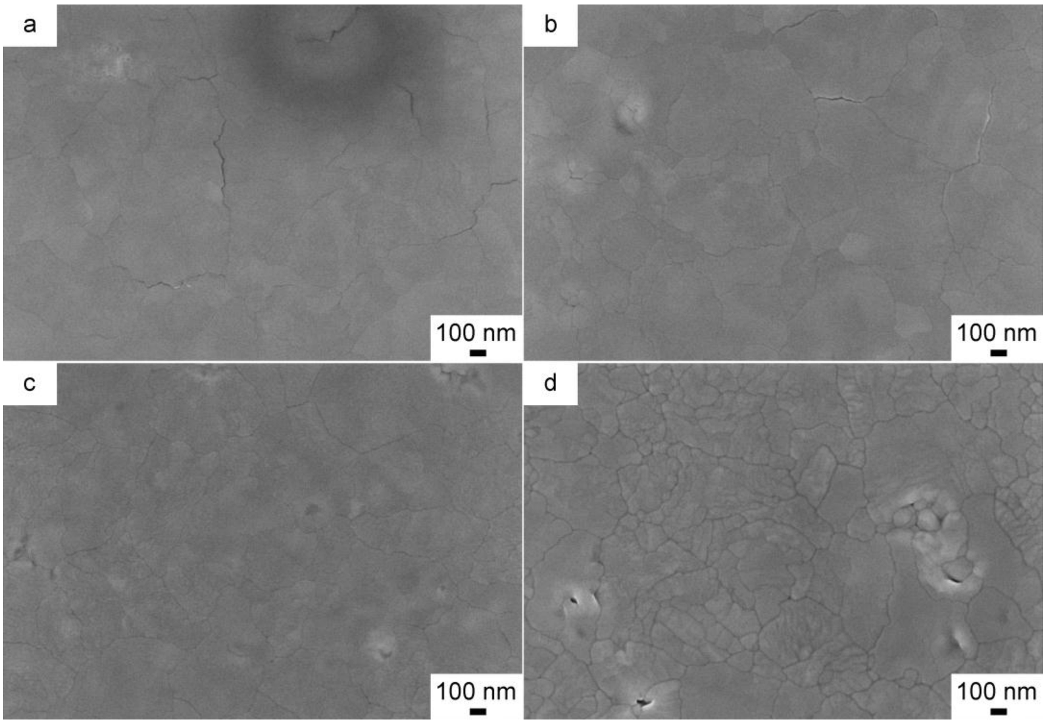

Fig. S2. SEM images of seed layers on FTO substrates spin coated with 0.5 mol L^{-1} colloid for three times and annealed at different temperatures: (a) 450 °C, (b) 500 °C, (c) 550 °C, (d) 600 °C.

Fig. S2 (a-d) shows the SEM images of the seed layers on FTO substrate spin coated with 0.5 mol L^{-1} colloid and annealed at different temperatures (450-600 °C). From Fig. S2 (a-d), it can be seen that the grain boundaries of the WO_3 nanoparticles become obviously discerned, indicating the WO_3 nanoparticles are crystallized gradually with the increasing of annealing temperature.

3. Effect of annealing time (seed layers)

Fig. S3 (a-c) shows the FESEM images of the seed layers of sample (a-c) with different annealing time. The morphologies of the three samples are not significantly different and the grain boundaries of seed layers of sample c may be clearer after careful comparison.

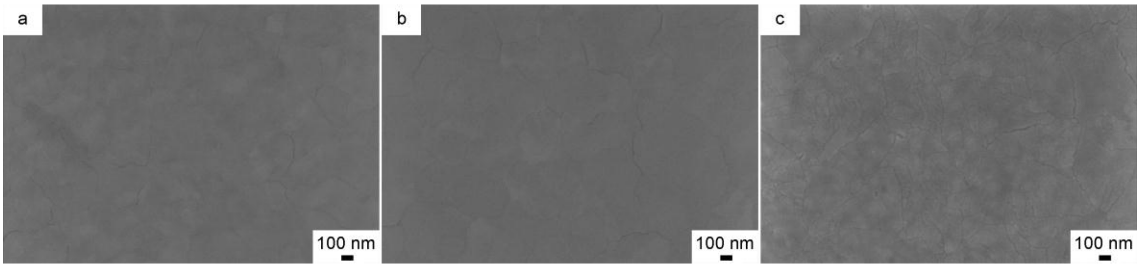

Fig. S3. SEM images of seed layers on FTO substrates spin coated with 0.5 mol L^{-1} colloid for three times, of which the annealing time were (a) 10, 10 and 10min, (b) 10, 10 and 30 min, (c) 10, 10 and 50 min, and the annealing processes were performed at 500 °C.

Fig. S4 (a-c) shows the XRD patterns of the seed layers of sample (a-c) with different annealing time. It is determined that all of the seed layers are monoclinic phase (JCPDS 01-072-1465). The relative intensive ratio of (202) peak over (200) peak of sample a is much lower than the other two samples.

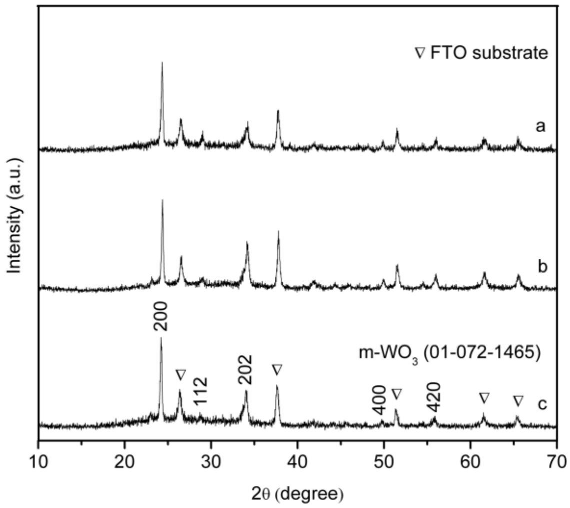

Fig. S4. XRD patterns of seed layers on FTO substrates spin coated with 0.5 mol L^{-1} colloid for three times, of which the annealing time were (a) 10, 10 and 10 min, (b) 10, 10 and 30 min, (c) 10, 10 and 50 min, and the annealing processes were performed at 500 °C.

4. Effect of concentration of colloid (seed layers)

Fig. S5 shows the FESEM images of seed layers on FTO substrates spin coated with different concentrations of H_2WO_4 colloid. At low concentration of H_2WO_4 colloid, the coated seed layers can't cover the FTO substrate completely and the edges of nano-particles of FTO substrate are observed clearly. With increasing the concentration of H_2WO_4 colloid, the thickness of the seed layers increases gradually, and the edges of nano-particles of FTO substrate decrease as shown in Fig. S5 (a-c). The FTO substrate is covered completely by seed layers in Fig. S5 (d) when the concentration of H_2WO_4 colloid increases to 0.5 mol L^{-1}.

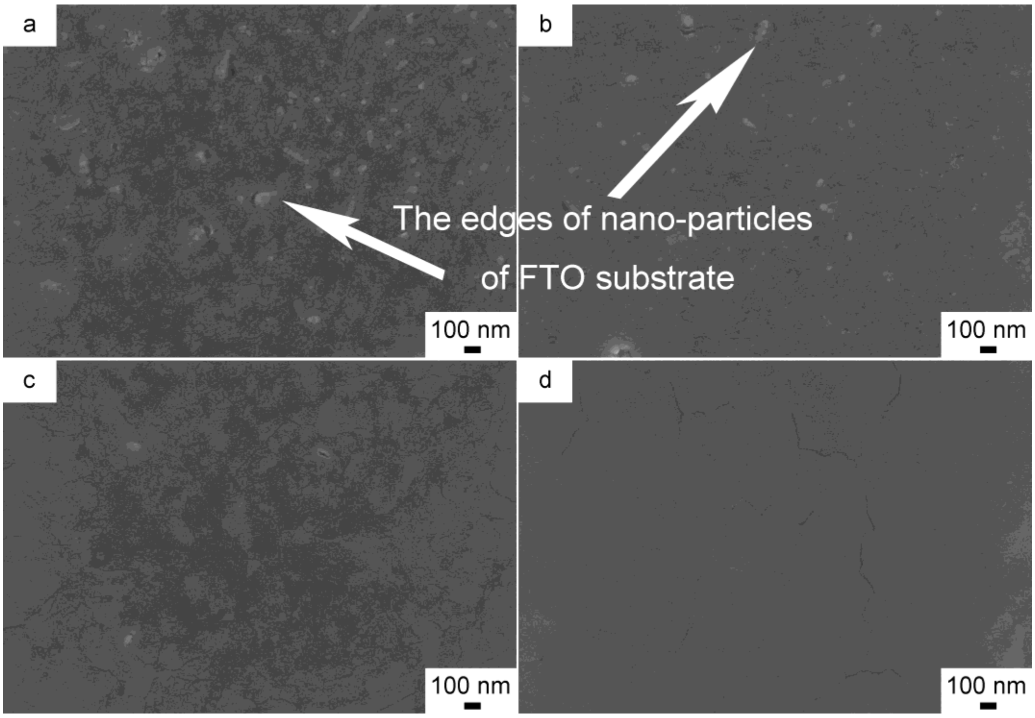

Fig. S5. SEM images of seed layers on FTO substrates spin coated with different concentrations of H_2WO_4 colloid: (a) 0.2 mol L^{-1}, (b) 0.3 mol L^{-1}, (c) 0.4 mol L^{-1}, (d) 0.5 mol L^{-1}.

Fig. S6 shows the XRD patterns of seed layers on FTO substrates spin coated with different concentrations of H_2WO_4 colloid. It is shown that diffraction peaks can be well indexed to the standard diffraction pattern of monoclinic phase WO_3 (JCPDS 01-072-1465). The relative intensive ratios of seed layers over FTO substrate are calculated by I_{200}/I_{FTO}, where I_{200} are the measured diffraction intensities due to (200) planes and I_{FTO} are the measured diffraction intensities appeared at 37.8°. And the values of the ratio are 0.759, 0.828, 1.401 and 1.488, respectively. This means that the numbers of the m-WO_3 seeds increase with the increasing concentration of H_2WO_4 colloid. The results of the XRD patterns of seed layers are in accord with SEM images in Fig. S5. The average particle diameters of the seed layers, D, are calculated using the Scherrer Equation: $D=K\lambda / B\cos\theta$, where K is a constant with a value of 0.89, λ is the wavelength of x-ray with a value of 0.154 nm, B is half-width of the diffraction peak and θ is the position of the diffraction peak. For WO_3 seed layers, the average particle diameters are calculated to be 35.9, 31.9, 34.5 and 35.9 nm, respectively, suggesting the sizes of WO_3 seeds keep nearly constant whether the concentration of H_2WO_4 colloid is higher or lower.

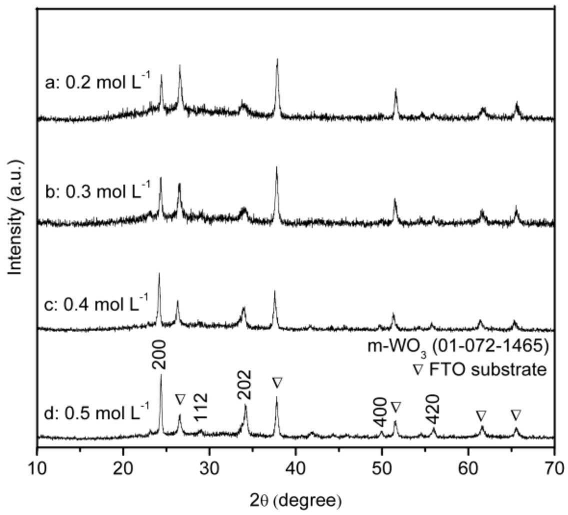

Fig. S6. XRD patterns of seed layers on FTO substrates spin coated with different concentrations of H_2WO_4 colloid: (a) 0.2 mol L^{-1}, (b) 0.3 mol L^{-1}, (c) 0.4 mol L^{-1}, (d) 0.5 mol L^{-1}.

5. Effect of spin-coated times

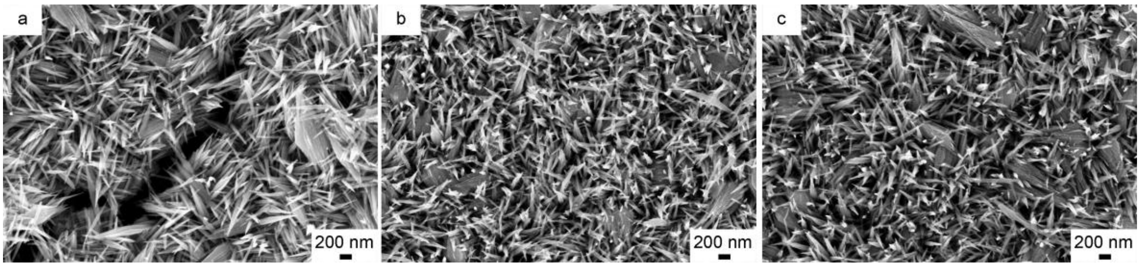

Fig. S7. SEM images of hydrothermal products grown on FTO substrates spin coated with 0.5 mol L^{-1} H_2WO_4 colloid for different times, of which the annealing time were (a) once for 30 min, (b) three times for 10, 10 and 30 min, (c) five times for 10, 10, 10, 10 and 30 min, and the annealing processes were performed at 500 °C.

The alternative method to change the number of the seeds is to change the spin-coated times on FTO substrates. Fig. S7 (a-c) shows the SEM images of hydrothermal products grown on FTO substrates spin coated with 0.5 mol L^{-1} H_2WO_4 colloid for once, three and five times. The main morphologies of the three samples are WNRs generally vertical to the substrates mixed with a few spindle-like nanorod bundles. However, when the substrate is spin coated once, the orientation of the WNRs is worse than that of the other two. And a number of micro-cracks also exist in the hydrothermal products, resulting in the products being detached easily from the FTO substrate. The products grown on the substrates spin coated for three and five times are generally in close contact with the substrates.

Fig. S8 (a-c) shows the XRD patterns of the hydrothermal products grown on FTO substrates spin coated with 0.5 mol L^{-1} H_2WO_4 colloid for once, three and five times. It can be seen that the hydrothermal products are hexagonal phase (JCPDS 00-033-1387). When the substrate is spin coated once, the strong back ground noise may come from the FTO substrate because a number of micro-cracks exist on it.

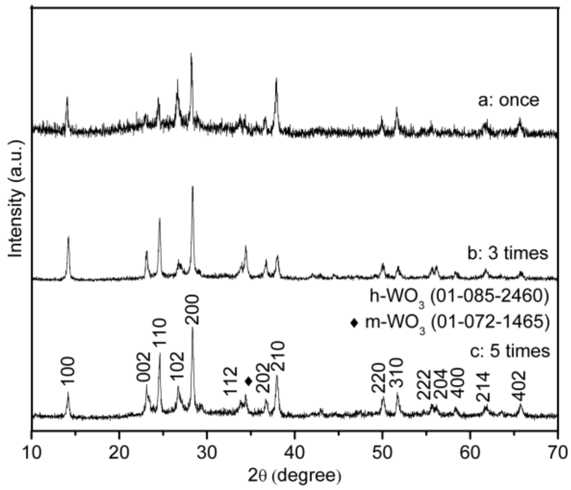

Fig. S8. XRD patterns of hydrothermal products grown on FTO substrates spin coated with 0.5 mol L^{-1} H_2WO_4 colloid for different times, of which the annealing time were (a) once for 30 min, (b) three times for 10, 10 and 30 min, (c) five times for 10, 10, 10, 10 and 30 min, and the annealing processes were performed at 500 °C.

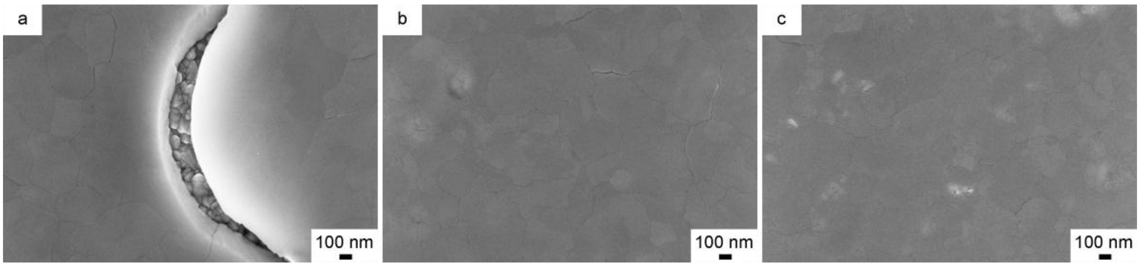

Fig. S9. SEM images of seed layers on FTO substrates spin coated with 0.5 mol L^{-1} H_2WO_4 colloid for different times, of which the annealing time were (a) once for 30 min, (b) three times for 10, 10 and 30 min, (c) five times for 10, 10, 10, 10 and 30 min, and the annealing processes were performed at 500 °C.

Fig. S9 (a-c) shows the SEM images of seed layers on FTO substrates spin coated with 0.5 mol L^{-1} H_2WO_4 colloid for different times. It can be seen from Fig. S9 (a) that a crack is observed clearly and the surface of FTO substrate is exposed when the FTO substrate is spin coated once. However, the other two substrates are covered completely by seed layers when spin coated three or five times as shown in Fig. S9 (b-c). This means that by increasing the spin-coated times, some cracks inevitable formed on the substrate spin coated for only once may be filled up with H_2WO_4 colloid solution, and an uniform thin film of WO_3 seed layer could be obtained when the substrate is annealed again. Therefore, the cracks are hard to be observed when the substrate is coated by H_2WO_4 colloid for several times.

Fig. S10 (a-c) shows the XRD patterns of seed layers on FTO substrates spin coated with 0.5 mol L^{-1} H_2WO_4 colloid for different times. The characteristic diffraction peaks of hexagonal WO_3 (01-072-1465) appear in these samples, whereas the relative intensive ratios of seed layers over FTO substrate are obviously different. And the values of the ratio I_{200}/I_{FTO} are 0.73, 1.488 and 4.045, where I_{200} are the measured diffraction intensities due to (200) planes and I_{FTO} are the measured diffraction intensities appeared at 37.8°. This means that the number of the m-WO_3 seeds formed on FTO substrates would increase with increasing spin-coated times with H_2WO_4 colloid. The results of the XRD patterns of seed layers are in accord with the SEM images in Fig. S9.

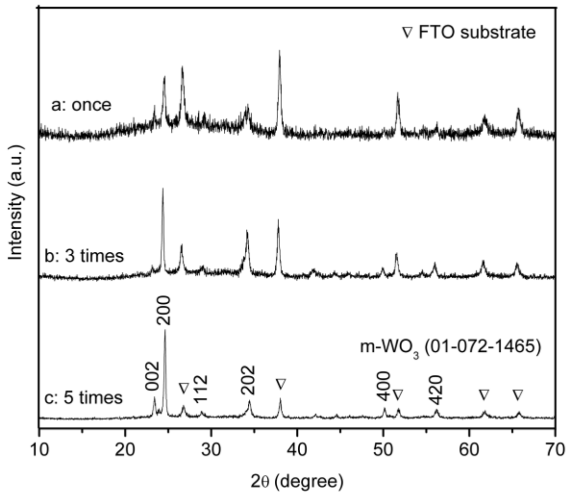

Fig. S10. XRD patterns of seed layers on FTO substrates spin coated with 0.5 mol L^{-1} H_2WO_4 colloid for different times, of which the annealing time were (a) once for 30 min, (b) three times for 10, 10 and 30 min, (c) five times for 10, 10, 10, 10 and 30 min, and the annealing processes were performed at 500 °C.

Based on the results and analysis above, it is confirmed that the number of the m-WO_3 seeds spin coated on FTO substrate could affect the morphologies of the final hydrothermal products. The number of the WO_3 seeds on FTO substrate spin coated once is less than that for several times, which result in poor orientation of formed WNRs. The micro-cracks existed in the hydrothermal products in Fig. S7 (a) might come from the cracks formed during annealing process as shown in Fig. S9 (a). It is also indicated that the cracks can be avoided by spin coating with H_2WO_4 colloid for several times.

6. Effect of increasing the spin-coated times when using low H_2WO_4 colloid concentration

Fig. S11 (a) shows the SEM images of WO_3 seed layers on the FTO substrate spin coated with 0.1 mol L^{-1} H_2WO_4 colloid for 10 times, and the annealing processes were performed at 500 °C. It can be seen that the WO_3 seeds can't cover the whole surface of FTO substrate completely even when the spin-coated times is 10, suggesting that the H_2WO_4 colloid concentration is too low. Fig. S11 (b-c) gives the SEM images of hydrothermal products grown on the pre-modified FTO substrate with low and high magnifications. Compared with the WNRs grown on the FTO substrate spin coated 3 times with 0.5 mol L^{-1} H_2WO_4 colloid, the WNRs with similar rod average diameter and high growth density were obtained. However, some micro-cracks also existed among the nanorods arrays, indicating that part of the FTO substrate surface was uncovered with WO_3 seed layers.

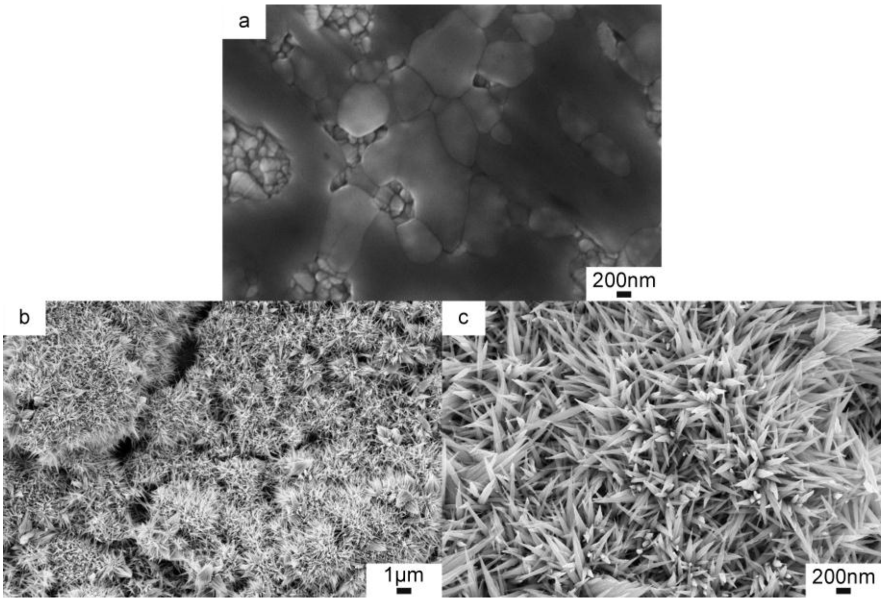

Fig. S11. (a) SEM images of seed layers on FTO substrate spin coated with 0.1 mol L^{-1} H_2WO_4 colloid for 10 times, and the annealing processes were performed at 500 °C; SEM images of hydrothermal products grown on the as-modified FTO substrate (b) with low magnification, (c) with high magnification.